

## Mechanisms of the Exchange of Diblock Copolymers between Micelles at Dynamic Equilibrium

Türkan Haliloğlu, İvet Bahar, and Burak Erman

*Polymer Research Center and School of Engineering, Bogazici University, and TUBITAK Advanced Polymeric Materials Research Center, Bebek 80815, Istanbul, Turkey*

Wayne L. Mattice\*

*Institute of Polymer Science, The University of Akron, Akron, Ohio 44325-3909*

*Received August 31, 1995; Revised Manuscript Received March 8, 1996*

**ABSTRACT:** The exchange dynamics of chains between micelles of diblock copolymers in dilute solution in a selective solvent has been studied by a semianalytical approach. A close inspection of dynamic Monte Carlo simulation trajectories showed that there are mainly two types of exchange mechanisms, chain insertion/expulsion and micellar merger/splitting. The relative contributions of the two mechanisms to the overall exchange dynamics are examined as a function of the following variables: the concentration of the diblock copolymers, the energy of interaction between the insoluble block and the surroundings, and the size of the insoluble block. A kinetic scheme, which incorporates the possible states of association and the mechanisms by which the exchange takes place, is constructed. The corresponding transition rates matrix, with the rate constants extracted from simulations, is used in a Master equation formalism to demonstrate that the two mechanisms involved in the exchange dynamics operate on time scales differing by at least 1 order of magnitude, in conformity with recent experimental observations. Application of a filtering technique to the transition rate matrix showed that the high-frequency modes of the relaxation are from the chain insertion/expulsion mechanism and the relatively slower modes, which dominate the tail parts of the time decay of correlation functions, are from the micellar merger/splitting type of transitions. The analysis thus provides an explanation for the two processes observed in the recent characterization of the exchange dynamics of chains between micelles by the efficiency of nonradiative singlet energy transfer. The chain insertion/expulsion mechanism is shown to be predominantly important at low concentrations and at high interaction energies between the insoluble block and the surroundings, while the micellar merger/splitting is activated at higher concentrations.

Diblock copolymers form micelles in dilute solution in liquids which are good solvents for one block but poor solvents for the other one. In a system of micelles of copolymers, the exchange dynamics of the chains between the micelles is an important dynamic property. An equilibrated system must be in a dynamic equilibrium, with pathways by which the micelles can exchange chains with one another. This phenomenon can be detected experimentally as a time dependence of the efficiency of nonradiative singlet energy transfer between micelles, which originally contain copolymers covalently labeled with a donor or with an acceptor exclusively, at the insoluble block or at the junction between the two blocks.<sup>1–3</sup> Exchange produces a population of micelles that contains both donor and acceptor. The nonexponential behavior observed in the time dependence of the intensity of the fluorescence makes difficult the interpretation of the easily measurable change in the intensity in terms of the microscopic rate constant of single chain insertion/expulsion from the micelle. Nevertheless, in the recent experimental analysis<sup>2</sup> of the chain exchange as monitored by nonradiative singlet energy transfer, it was concluded that the formation of mixed micelles of two differently labeled copolymers in the experiments may be influenced by another process in addition to the transfer of a single chain from one micelle to the other via the pool of free chains. A similar study has also been carried out by Procházka et al.<sup>1</sup> Sedimentation velocity has also been used to investigate the exchange dynamics, and a qualitative description of the dynamics has been provided.<sup>4</sup>

On the theoretical side, Halperin and Alexander<sup>5</sup> have given a theoretical description of the relaxation dynamics of the micelles using the chemical relaxation technique. They concluded that the only mechanism which is dominant in the exchange should be the Aniansson–Wall mechanism.<sup>6</sup> In this model, the micellar size distribution is adjusted in steps consisting of chain insertion/expulsion, which has the lowest activation energy. The proper rate-limiting quantities are identified by a set of reactions which define the association (and dissociation) in unitary steps. However, the chemical reaction method is not very useful in the study of the dynamic equilibrium of polymeric micelles<sup>7</sup> due to the large perturbation of the system required for a detectable change. The analysis of Halperin and Alexander assumes a small perturbation of the system from equilibrium.

The exchange of the chains is also detected in the dynamic Monte Carlo (MC) simulations as small fluctuations in the fraction of the chains that exist as free chains.<sup>8</sup> Dynamic MC simulations have the potential for showing how the variables in the system affect the time scale and heterogeneity of the relaxation, as well as the mechanisms by which the micelles exchange chains with one another.<sup>9,10</sup> The correlation curves describing the dynamics of the exchange may be very different in form from a single exponential, with very long tails expected. Evaluation of the relaxation time by simply evaluating the area under the curve in the conventional way is difficult, due to the long tails.

In the present work, we attempt another type of analysis to study the dynamics of the exchange. It starts with the identification of the mechanisms involved in the chain exchange and their relative contri-

\* Abstract published in *Advance ACS Abstracts*, May 1, 1996.

**Table 1. Number-Average and Weight-Average Molecular Weights, as  $M_n/M_0$  and  $M_w/M_0$ , of the Aggregates; the Correlation Times,  $\tau_c$ , Corresponding to the  $1/e$  Decay of the Correlation Function  $R(t)$  (in  $10^2$  MC Steps); and the Compactness of the Cores,  $\theta$ , for the Systems Studied<sup>a</sup>**

$\phi$	$e$	$N_A$	$M_n/M_0$	$M_w/M_0$	$\tau_c$			$\theta$
					both	I/E	MM/S	
0.02	0.45	10	4.24	8.08	41	55	292	0.22
0.03	0.45	10	7.43	16.81	76	108	438	0.31
0.05	0.45	10	10.89	22.87	80	199	169	0.41
0.08	0.45	10	17.26	26.65	105	240	248	0.51
0.1	0.45	10	18.40	30.48	59	278	95	0.54
0.05	0.43	10	8.98	21.04	45	101	101	0.31
0.05	0.45	10	10.89	22.87	80	199	169	0.41
0.05	0.48	10	22.33	33.42	292	410	1200	0.56
0.05	0.375	12	4.85	9.48	16	32	35	0.013
0.05	0.45	10	10.89	22.87	80	199	169	0.41
0.05	0.563	8	16.95	22.55	184	350	530	0.51
0.05	0.75	6	16.90	19.27				0.61

<sup>a</sup>  $N_B = 10$ .

contributions to the overall dynamics. For that purpose, trajectories of each tracer chain over a long time span are analyzed. The resulting picture gives us an insight into which can be used to formulate a model to describe the mechanisms by which the chain exchange occurs. A kinetic scheme is constructed accordingly, and the transition rate matrix, **A**, which governs the exchange dynamics following a master equation formalism is formed based on the kinetic scheme. The exchange of the chains from the solution of the master equation is studied as a function of different system variables; concentration, composite variable of interaction energy and size of insoluble block, and interaction parameter.

The forthcoming sections can be summarized as follows: The simulation method will be described briefly. The transitions deduced directly from the simulations will be presented, along with the classification of the processes and the transition rates. The master equation formalism, which proved useful in exploring the conformational dynamics of the polymers,<sup>11,12</sup> will be adopted for the theoretical analysis of the exchange dynamics. And the results of the calculations based on the solution of the master equation will be presented and discussed.

## Method

The structure of the chains is  $A_{N_A}-B_{N_B}$ , where  $N_A$  and  $N_B$  are the lengths of blocks A (insoluble) and B (soluble), respectively. The simulations are run on a  $60^3$  cubic lattice with periodic boundary conditions in all three directions for the systems listed in the first three columns of Table 1. Lattices of other sizes are used to check for the absence of size effects.  $\phi$  is the volume fraction of diblocks in the cubic box. The empty sites are occupied by the solvent, S. The reduced pairwise interaction parameter  $e_{XY}$ , which is proportional to the Flory-Huggins interaction parameter  $\chi$ , is applied to the pairs of species X and Y, whenever they are nonbonded but are nearest neighbors on the lattice. We employ  $e_{AB} = e_{AS} > 0$ , with all other  $e_{XY} = 0$ . Henceforth, the nonzero  $e_{XY}$  will be denoted simply by  $e$ . The values adopted for  $e$  in the present simulations are listed in the second column of Table 1. Extended Verdier-Stockmayer moves<sup>13</sup> are used to convert one replica into another. The Metropolis rule<sup>14</sup> is applied for acceptance of a new replica.

The diblock chains are initially generated as parallel rods and then randomized by running the simulation with  $e = 0$ . The interaction energies are then turned on, and the system is again allowed to come to equilibrium. The equilibrium is determined by the stabiliza-

tion of the fraction of free chains and the weight-average sizes of the aggregates. After equilibrium, the simulations are run long enough to observe the dynamic equilibrium of the system. The long-term dynamics is deduced from a long series of snapshots. Successive snapshots are separated by 100–120 Monte Carlo (MC) time steps, depending on the trajectory. One Monte Carlo step is defined as the number of iterations that would have moved  $(N_A + N_B)N_c$  beads, if every move were accepted.  $N_c$  is the number of chains in the periodic box and varies in the range  $216 \leq N_c \leq 1100$ . A more detailed description of the method can be found in refs 9 and 10.

## Transitions Deduced Directly from the Simulations

In order to gain insight into the mechanisms of exchange, a direct analysis of the dynamic simulation trajectories has been carried out. The analysis is based on following each individual chain in the system through a long time span.

**Classification of Processes.** Inspection of the dynamic equilibrium for the diblock copolymers in the presence of a selective solvent reveals three distinct types of exchange mechanisms. The transition states for these exchange mechanisms are sketched in Figure 1.

**(i) Chain Insertion/Expulsion.** A chain is expelled by a micelle, exists for at least one (or two) snapshot as a free chain, and later is captured by a different (or the same) micelle. A transition state, showing the free chain between two micelles, is depicted in Figure 1a. The requirements stated in parentheses in the opening sentence of this definition exclude the process by which a chain is expelled from a micelle and immediately recaptured by the same micelle.

**(ii) Micellar Merger/Splitting.** The number of chains in a micelle changes from  $m$  to  $m + \Delta m$  and remains at  $m + \Delta m$  for at least two successive snapshots. The value of  $\Delta m$  cannot be  $-1$ ,  $0$ , or  $1$ . Two micelles merge if  $\Delta m > 1$ , and a micelle splits if  $\Delta m < -1$ . This mechanism is depicted in Figure 1b, showing two micellar cores in contact and a chain that is part of both cores. When the two micellar cores separate, the labeled chain must become a part of one micelle or the other but can no longer belong to both micelles.

**(iii) Micellar Spanning.** When the exteriors of the cores of two independent micelles are separated by less than the fully extended length of an A block, a chain can transfer from one micellar core to the other micellar

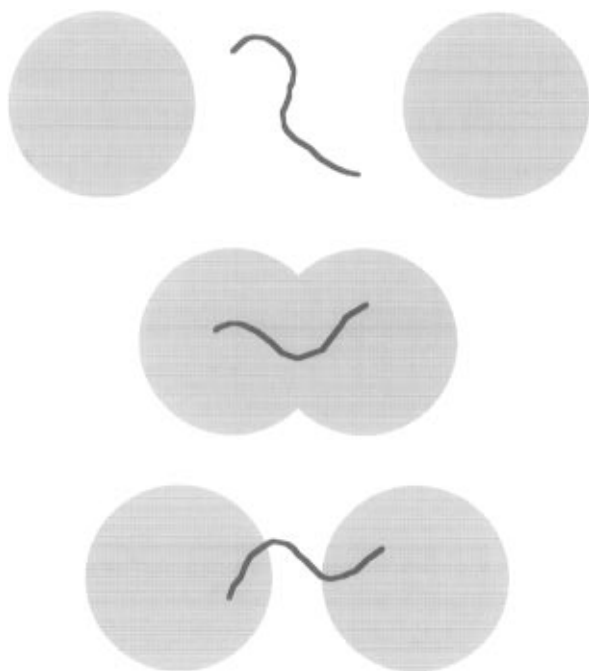


**Figure 1.** Sketch of the transition states in (a, top) chain insertion/expulsion, (b, middle) micellar merger/splitting, and (c, bottom) micellar spanning.

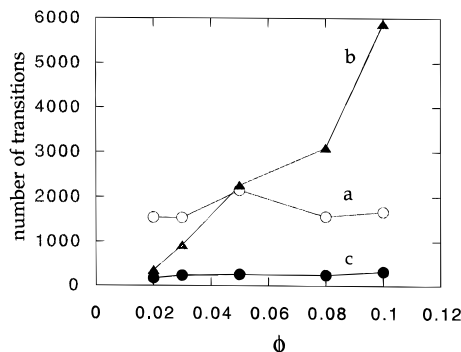


**Figure 2.** Number of transitions via (a) chain insertion/expulsion, (b) micellar merger/splitting, and (c) micellar spanning during 35 482 Monte Carlo steps. Each block contains 10 beads and  $e = 0.45$ .

core without ever becoming a free chain. This mechanism is sketched in Figure 1c. A chain is migrating from one micellar core to another without becoming a free chain and without contact of the cores. Micellar spanning is assumed to have occurred if the tracer chain transfers from one micelle to another by a process that does not fulfill the requirements for insertion/expulsion or for merger/splitting.

**Transition Rates.** A preliminary description of the transition rates has been presented.<sup>15</sup> The transition rates are proportional to the number of events per unit time. The rates for chain insertion/expulsion, micellar merger/splitting, and micellar spanning were evaluated directly from the dynamic MC simulations, by simply counting the number of transitions of each type that are observed in a specified number of MC steps. An example of the results is depicted in Figure 2 for simulations in which the critical micelle concentration (cmc) is 0.008, as shown in an earlier work.<sup>8</sup> Here,  $N_A = 10$  and  $e = 0.45$ . The trajectory is long enough so that there is an average of seven to nine transitions per chain. Chain insertion/expulsion is the dominant mechanism when  $\phi$  is slightly above the cmc. At these concentrations, a large fraction of the diblock copolymer

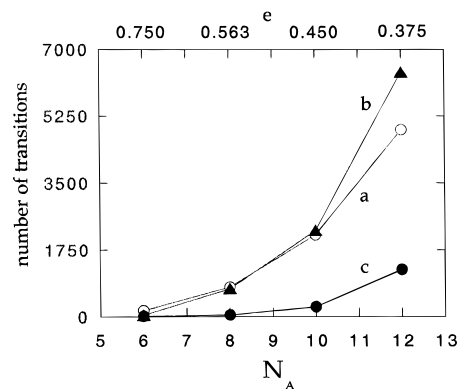


**Figure 3.** Number of transitions via (a) chain insertion/expulsion, (b) micellar merger/splitting, and (c) micellar spanning during 35 482 Monte Carlo steps.  $\phi = 0.05$ ,  $N_B = 10$ , and  $N_A e = 4.5$ .

is present as free chains, and the exchange mechanism that utilizes the free chains is the one that is dominant. The number of transitions that occur by chain insertion/expulsion is nearly independent of  $\phi$  for the range covered in Figure 2, perhaps because the concentration of free chains,  $\phi_{\text{free}}$ , is nearly constant ( $\phi_{\text{free}} = 0.0084 - 0.0064$ , from the lowest to the highest concentration).

In contrast, the number of transitions in Figure 2 that occur via micellar merger/splitting increases strongly as  $\phi$  becomes larger. The number density of micelles becomes larger as  $\phi$  rises above the cmc, and the likelihood of close encounters between pairs of micelles increases as the square of the number density. As a consequence, micellar merger/splitting becomes the dominant mechanism of exchange at higher concentrations. In the conditions used for the simulations, there is a comparable number of exchanges via chain insertion/expulsion and micellar merger/splitting when the concentration is about 10 times the cmc.

The composite variable  $eN_A$  has been proposed to be a parameter controlling the equilibrium properties, such as the morphology of self-assembled block copolymers.<sup>16</sup> If this composite variable also controls the dynamics, in this case, the transitions should be unaffected by an increase in  $N_A$  by a factor of  $x$ , provided that  $e$  is decreased by the same factor,  $eN_A = (e/x)(xN_A)$ . The actual behavior observed in the dynamic MC simulations is depicted in Figure 3. The transition rates for all three mechanisms are slower at small  $N_A$  and large  $e$  than they are at large  $N_A$  and small  $e$ , even though the product  $eN_A$  is held constant at 4.5. The system is almost frozen at the largest  $e$  used, with the average number of transitions per chain being well below 1. Clearly,  $eN_A$  is not a useful variable in characterizing the transition rates. The changes in  $e$  dominate the reciprocal changes in  $N_A$ .

The influence of  $e$  itself on  $A_{10}B_{10}$ , at  $\phi = 0.05$ , is depicted in Figure 4. The average number of transitions per chain ranges from 3 to 11 in these trajectories. The transition rates for all three mechanisms decrease as the interaction energy becomes stronger, as expected. The larger energy makes chain expulsion more difficult because the A block experiences a stronger energetic penalty when it is exposed to solvent. The larger energy also improves the organization of the cores of the micelles, causing them to approach more closely a classic core-shell structure. This improvement in the organization of the micelles makes direct micelle-micelle interactions more difficult, due to the repulsions of the corona of the two micelles. The corona in the classic

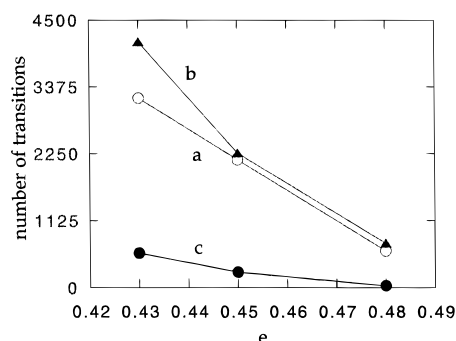


**Figure 4.** Number of transitions via (a) chain insertion/expulsion, (b) micellar merger/splitting, and (c) micellar spanning during 35 482 Monte Carlo steps.  $\phi = 0.05$ , and  $N_A = N_B = 10$ .

core-shell model is formed by blocks of B that are swollen by the solvent. The increase in the organization of the core with increasing  $e$  accounts for the increase in  $\theta$ , reported in the last column of Table 1. Here  $\theta$  is the fraction of the nonbonded neighbors of A that are also A. While the values of  $\theta$  increase as  $e$  increases, they remain well below the value of  $\approx 0.99$  expected for a perfect core-shell micelle with about 20 chains of  $A_{10}B_{10}$ . This value of  $\theta$  might be approached at larger  $e$ , but then the system would become frozen on the time scale of the simulation.

Micellar spanning accounts for only a small fraction of the transitions under all conditions examined, as is apparent in Figures 2–4. The simulations suggest that it would be almost inconsequential to ignore micellar spanning entirely and construct a theoretical analysis based on the transition rates for chain insertion/expulsion and micellar merger/splitting only. The theoretical analysis, based on the master equation, using the transition rates for chain insertion/expulsion and micellar merger/splitting, is presented in the following sections.

### Kinetic Scheme

Examination of MC trajectories leads us to construct the following kinetic scheme to describe the mechanisms of the exchange of chains between micelles at the dynamic equilibrium. The micellar merger/splitting type of transitions imply the consideration of the tracer chain in the aggregates of different sizes. Merging and splitting are therefore analyzed as a function of the size of the aggregate with which the tracer chain is associated. In addition to that, having a state of being a free chain enables us to account for the exchanges via the free chain.

Ideally, we should consider separately micelles of every size. This ideal approach is not practical because the number of states would be huge and the statistical uncertainties in the transition rates between all pairs of states would be enormous. Therefore, we reduce the number of micellar states to three. These are denoted as S (small), M (medium), and L (large) depending on the size of the aggregate, whereas free chains are designated as F. The resulting kinetic scheme is given by Figure 5. The size range (in number of chains) attributed to each class of aggregates is characterized by the number-average and the weight-average molecular weights,  $M_n$  and  $M_w$ , of the aggregates for a given system. Table 1 gives  $M_n/M_0$  and  $M_w/M_0$  values, where  $M_0$  is the mass of a single chain, for various systems simulated in the present study. Being a good measure

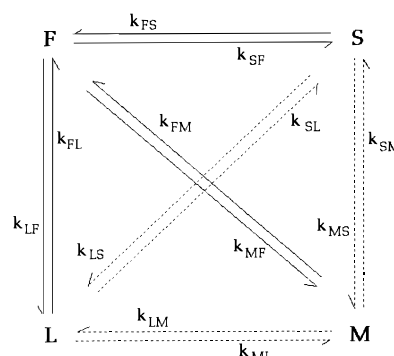


**Figure 5.** Kinetic scheme constructed based on the transitions observed from dynamic simulation trajectories.

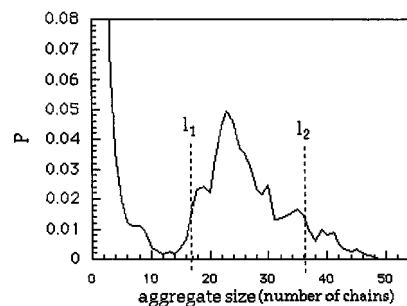


**Figure 6.** Aggregate size distribution for a system of  $\phi = 0.08$ ,  $e = 0.45$ , and  $N_A = N_B = 10$ .  $M_n/M_0 = 17.26$  and  $M_w/M_0 = 26.65$ .

of the average size and polydispersity of the aggregates, they help to draw the limits for the specification of the aggregate size in terms of the number of chains included in the aggregate. Accordingly, the lower and upper limits for the size  $s(M)$  of aggregates of type M are set by the respective values of  $l_{1,2} = 1/M_0(M_w \pm (M_w - M_n))$ . Therefore,  $s(F) = 1$ ,  $1 < s(S) < l_1$ , and  $s(L) > l_2$ . The  $l_1$  and  $l_2$  values have been observed to be in the respective ranges of 4–22 and 12–45 for the different systems that are discussed here. Figure 6 depicts the aggregate size distribution for the case  $\phi = 0.08$ ,  $e = 0.45$ , and  $N_A = N_B = 10$ . For that specific system,  $M_n/M_0 = 17.26$  and  $M_w/M_0 = 26.65$ . The limits  $l_1$  and  $l_2$  are shown by the vertical dashed lines on the figure.

The solid and dashed arrows on the kinetic scheme in Figure 5 denote the chain insertion/expulsion and micellar merger/splitting processes, respectively. Thus, if the exchange occurs through the solid arrows, chain insertion/expulsion is observed; otherwise, micellar merger/splitting operates for the exchange. The transition rates based on the above kinetic scheme have been directly calculated from the dynamic simulation trajectories and inserted in the transition rate matrix of the master equation formalism.

### Master Equation Formalism

The dynamic space is composed of four states (F, S, M, L) and two types of mechanisms by which the transition occurs between those states. The stochastic process of transitions between those states is described by the master equation

$$d\mathbf{P}(t)/dt = \mathbf{A}\mathbf{P}(t) \quad (1)$$

where the vector  $\mathbf{P}(t)$  represents the array of the instantaneous probabilities of the four states and  $\mathbf{A}$  is the  $4 \times 4$  transition rate matrix. Let the indices  $a, b, \dots, N$  indicate the defined states accessible to any tracer

chain in the system. The off-diagonal element  $k_{ab}$  of  $\mathbf{A}$  is the rate constant for the transition from state  $b$  to state  $a$  by the direct path already defined in the kinetic scheme. The diagonal elements  $k_{aa}$  are given by

$$k_{aa} = -\left(\sum_{b \neq a} k_{ba}\right) \quad (2)$$

where the summation is performed over all  $b \neq a$  so that the sum of the elements in each column is zero. The rate matrix,  $\mathbf{A}$ , is written as

$$\mathbf{A} = \begin{bmatrix} k_{FF} & k_{FS} & k_{FM} & k_{FL} \\ k_{SF} & k_{SS} & k_{SM} & k_{SL} \\ k_{MF} & k_{MS} & k_{MM} & k_{ML} \\ k_{LF} & k_{LS} & k_{LM} & k_{LL} \end{bmatrix} \quad (3)$$

Here, the six off-diagonal terms in the first row and the first column refer to chain insertion/expulsion types of transitions, and the remaining six off-diagonal terms correspond to micellar merger/splitting types of transitions.

The formal solution to eq 1 is

$$\mathbf{P}(t) = \exp(\mathbf{A}t)\mathbf{P}(0) = \mathbf{B} \exp(\Lambda t)\mathbf{B}^{-1}\mathbf{P}(0) \quad (4)$$

Here  $\mathbf{B}$  and  $\Lambda$ , obtained from the diagonalization of  $\mathbf{A}$ , are the matrix of the eigenvectors and the diagonal matrix of the eigenvalues, respectively.  $\mathbf{B}^{-1}$  is the inverse of  $\mathbf{B}$ . The product  $\mathbf{B} \exp(\Lambda t)\mathbf{B}^{-1}$  is the transition or conditional probability matrix,  $\mathbf{C}(t)$ , the elements of which are given as

$$C_{ab}(t) = \sum_k B_{ak} \exp(\lambda_k t) B_{kb}^{-1} \quad (5)$$

Here  $\lambda_k$  is the  $k$ th element of  $\Lambda$ . From eq 5, it is possible to obtain the time-dependent conditional probability of occurrence of state  $a$  for a given chain that originally is in state  $b$ .  $C_{ab}(t)$  incorporates both types of mechanisms and all the transition paths in between those two states, for the given time. The following correlation function is defined to have an overall view of the exchange dynamics:

$$R(t) = \frac{\sum_{i=1}^4 N_{i,0} C_{ii}(t)}{\sum_{i=1}^4 N_{i,0}} \quad (6)$$

Here the summations are performed over all possible states: F, S, M, and L.  $N_{i,0}$  is the equilibrium number of chains in state  $i$ .  $C_{ii}(t)$  is the conditional probability of being in state  $i$  after a time interval  $t$ , for a chain originally in state  $i$ .

### Calculations

**Eigenvalues.** The transition rate matrix,  $\mathbf{A}$ , is constructed according to the kinetic scheme described above as a function of different variables (concentration, interaction parameter, block size) effective in the exchange dynamics. The eigenvalues obtained from the solution of the master equation are depicted in Figure 7. One of the eigenvalues is identically equal to zero, and the remaining three are shown as a function of  $\phi$ ,

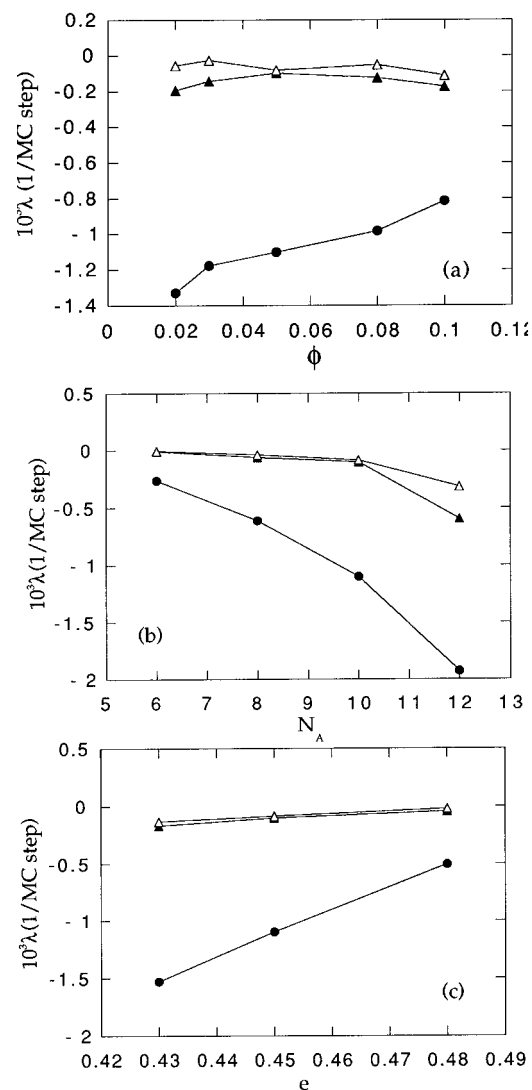


**Figure 7.** Eigenvalues,  $\lambda_k$ , (a) as a function of concentration,  $\phi$ ,  $e = 0.45$ , and  $N_A = N_B = 10$ , (b) for systems at composite variable  $eN_A = 4.5$ ,  $\phi = 0.05$ , and  $N_B = 10$ , and (c) as a function of the interaction parameter,  $e$ ,  $\phi_{\text{total}} = 0.05$ , and  $N_A = N_B = 10$ .

$N_A$ , and  $e$ , in parts a, b, and c, respectively, of Figure 7. The set of four eigenvalues for each system variable describes the stochastics of the transitions between the possible states for the tracer chain. Their absolute values may be identified as the frequencies of the individual modes contributing to chain exchange dynamics. In all cases, the three nonzero eigenvalues are on basically two time scales, differing by an order of magnitude. The difference diminishes as the concentration  $\phi$  of diblocks increases, as the interaction parameter increases, and as the size of the insoluble block becomes smaller. As we shall see later, the largest eigenvalue is dominated with the transitions associated with F. The other, slower two eigenvalues have their predominance coming from micellar merger/splitting types of transitions and are about of the same magnitude. On the premise of the above argument, it is interesting to note that different states other than F have about the same contribution to the stochastics of the transitions. The connection between the real states and the eigenstates will be elucidated in detail below.

**Correlation Functions.** The correlation function,  $R(t)$ , defined by eq 6 is calculated for the systems at different concentrations, at the composite variable of the

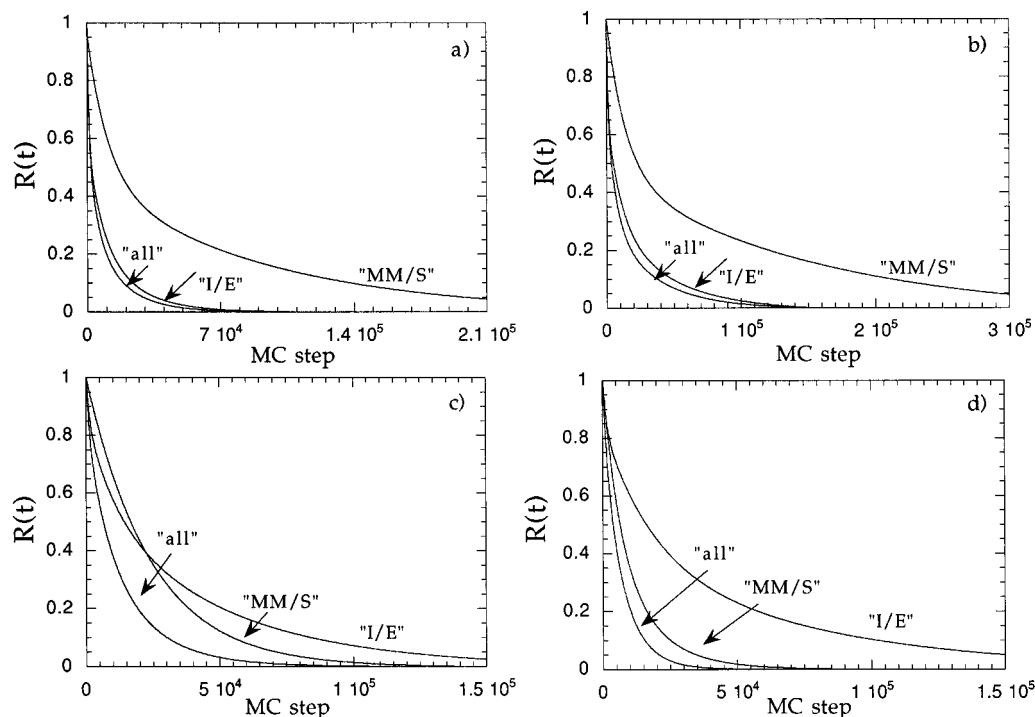


**Figure 8.** Correlation function,  $R(t)$ , calculated by using the transition rate matrices  $\mathbf{A}$ ,  $\mathbf{A}'$ , and  $\mathbf{A}''$  which respectively includes both chain insertion/expulsion and micellar merger/splitting mechanisms (all), only the chain splitting/expulsion mechanism (I/E), and only the micellar merger/splitting (MM/S) mechanism, as a function of concentration: (a)  $\phi = 0.02$ , (b)  $\phi = 0.03$ , (c)  $\phi = 0.08$ , (d)  $\phi = 0.1$ .  $e = 0.45$  and  $N_A = N_B = 10$ .

interaction parameter and block size (insoluble), and at different interaction parameters. The resulting normalized curves are labeled as all in Figure 8 and as both in Figure 9. Parts a–d in Figure 8 refer to various concentrations at fixed  $e$  and  $N_A$ . In Figure 9, on the other hand, parts a–d describe the effect of varying the interaction parameters at fixed  $\phi$  and  $N_A$ . To understand the relative contributions of the two different mechanisms, chain insertion/expulsion and micellar merger/splitting, to the chain exchange dynamics, the following filtering process is also applied to the transition rate matrix:

(i) Let the only operating mechanism be chain insertion/expulsion. The objective requires exclusion of all the terms describing the micellar merger/splitting in matrix  $\mathbf{A}$  and keeping the rest for chain expulsion. The modified transition rate matrix,  $\mathbf{A}'$ , is

$$\mathbf{A}' = \begin{bmatrix} k_{FF}' & k_{FS} & k_{FM} & k_{FL} \\ k_{SF} & k_{SS}' & 0 & 0 \\ k_{MF} & 0 & k_{MM}' & 0 \\ k_{LF} & 0 & 0 & k_{LL}' \end{bmatrix} \quad (7)$$

The correlation functions  $R(t)$  computed using  $\mathbf{A}'$  are denoted as I/E in Figures 8 and 9.

(ii) Let the micellar merger/splitting type of mechanism operate and suppress any exchange via the pool of free chains. The transition rate matrix,  $\mathbf{A}''$ , is

$$\mathbf{A}'' = \begin{bmatrix} 0 & 0 & 0 & 0 \\ 0 & k_{SS}'' & k_{SM} & k_{SL} \\ 0 & k_{MS} & k_{MM}'' & k_{ML} \\ 0 & k_{LS} & k_{LM} & k_{LL}'' \end{bmatrix} \quad (8)$$

The curves computed using  $\mathbf{A}''$  are denoted by MM/S in Figures 8 and 9.

The correlation times corresponding to the  $1/e$  decays of the curves are listed in Table 1. From those curves, it is interesting to note the following observations:

**Effect of Concentration.** By means of the filtering process applied to  $\mathbf{A}$ , it is easy to see which type of mechanism is controlling the overall chain exchange at different concentrations. At the lower concentrations, chain insertion/expulsion is dominant, and at the higher concentrations, micellar merger/splitting takes over. For example, at  $\phi = 0.02$ , the decay of  $R(t)$  (all in Figure 8a) is successfully reproduced by considering only the chain insertion/expulsion type of transitions (I/E). On the other hand, at  $\phi = 0.1$ , the dominant process is the micellar merger/splitting type (MM/S in Figure 8d). The ratio of the correlation time,  $\tau_c$ , of chain insertion/expulsion to that of micellar merger/splitting is 0.19 for the former case and 2.9 for the latter (see Table 1). At intermediate concentrations, both processes are contributing. The last column of Table 1 reports the average fraction of nonbonded nearest-neighbor sites of an A bead that are occupied by another A bead. This number rises as  $\phi$  increases, showing that the cores of the micelles are becoming larger, as shown also by changes in  $M_n/M_0$  and  $M_w/M_0$ .

As a general observation, chain insertion/expulsion is responsible for the initial decay at almost all the concentrations where the simulations are carried out. The portion of the decay described by chain insertion/expulsion decreases as  $\phi$  increases, ranging from almost the entire decay at  $\phi = 0.02$  to only the very earliest portion at  $\phi = 0.1$ . Chain insertion/expulsion leads to the relatively higher frequency modes of the relaxation, and micellar merger/splitting type chain exchange determines the relaxation of the tail parts of the correlation function  $R(t)$ . Apparently, the longer lifetimes belong to those chains undergoing micellar merger/splitting type transitions. So, longer lifetimes do not necessarily mean a smaller number of transitions,

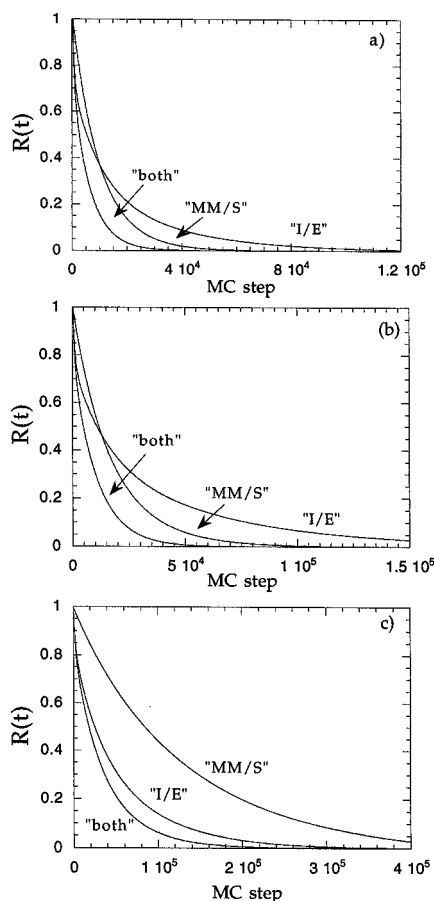


**Figure 9.** Correlation function,  $R(t)$ , calculated by using the transition rate matrices  $\mathbf{A}$ ,  $\mathbf{A}'$ , and  $\mathbf{A}''$  which respectively include both chain insertion/expulsion and micellar merger/splitting mechanisms (both), only the chain insertion/expulsion mechanism (I/E), and only the micellar merger/splitting (MM/S) mechanism, as a function of interaction parameter: (a)  $e = 0.43$ , (b)  $e = 0.45$ , (c)  $e = 0.48$ .  $\phi = 0.05$  and  $N_A = N_B = 10$ .

depending on the population of the chains undergoing the process in question.

**Effect of Interaction Parameter.** Figure 9 depicts the correlation curves calculated as based on  $\mathbf{A}$ ,  $\mathbf{A}'$ , and  $\mathbf{A}''$  for a system at a given concentration and block size but at different interaction parameters to see solely the effect of the interaction parameter. At the highest interaction parameter,  $e = 0.48$ , the primary exchange mechanism is chain expulsion. Apparently, the high  $e$  value leads to the formation of very well-defined core-shell micelles among which it is harder to expect micelle-micelle interactions rather than any exchange by chain insertion/expulsion. This suggestion is supported by the degree of compactness described by  $\theta$  (Table 1). At the lower interaction parameters, contributions from both types of transitions are important. The high-frequency modes of the relaxation are coming from chain insertion/expulsion, and the relaxation of the tails of the correlation curve, which is the relatively slower mode of the observed dynamics, is the result of micellar merger/splitting.

### Connection with Fluorescence Experiments

Figures 4 and 9 are pertinent to the interpretation of experiments which investigate the dynamics of the exchange of chains between micelles, using the efficiency of nonradiative singlet energy transfer and labeled chains.<sup>1-3</sup> If the solvent is very poor for the insoluble block, no exchange can be observed in the

experiment. This condition corresponds to the simulations when  $e > 0.5$ , where the dynamics is shut down (see Figure 4). In order to provide an exchange on a measurable time scale, the experimentalist can move to another medium that is less hostile to the insoluble block. This change in the experiment corresponds to selecting  $e < 0.5$  in the simulations. There is only a very narrow window for  $e$  (at about  $0.48 \pm 0.02$  in the simulations) where the exchange occurs at a measurable rate and is dominated by insertion/expulsion. At smaller  $e$ , the rate of exchange is still easily measurable, but both insertion/expulsion and merger/splitting become important. Since the experimentally measured exchanges have been described empirically by two processes with rather different time constants, we suspect that the experiments were performed in this regime. In order to produce dynamics on a convenient time scale, the experimentalists selected solvents that are not in the narrow range where insertion/expulsion completely dominates the exchange but instead selected less poor solvents for the insoluble block, thereby activating merger/splitting as well as insertion/expulsion. The faster process detected in the experiment can be identified with insertion/expulsion. This identification of the origin of the fast process was not possible from experiment alone but is possible when the simulations are analyzed in the manner depicted in Figures 8 and 9.

The merger/splitting becomes activated at the smaller  $e$  values because the core no longer has a sharp interface but instead has a dynamically active, fuzzy interface, in which many chains continually make unsuccessful attempts to escape the core (and a few succeed in escaping as free chains). It is the encounters of two micelles with these dynamically active, fuzzing interfaces that are responsible for the exchange of chains via merger/splitting. Of course, since we cannot perform simulations for systems where the blocks are very large, we cannot say how the results reported here for relatively small diblock copolymers might be related to systems containing much longer chains.

### Concluding Remarks

We concentrated on the identification of the mechanisms involved in exchange of the chains between the micelles of diblock copolymers. The dynamic analysis of the exchange by the master equation formalism, which utilizes the transition rate matrix based on the kinetic scheme constructed according to the observations from dynamic MC trajectories, led to results which might explain the observations in the fluorescence experiments. A semianalytical approach is very convenient to study the dynamics in a very compact analytical form, while having the feedbacks for the stochasticity of the transitions, which govern the analytical solution, from the simulations. Observation of the simulated system from a Monte Carlo time window, inasmuch as it is sufficient to catch the behavior of the system, permits the projection of that behavior to longer times. The following observations have been obtained from the calculations:

There are basically two types of mechanisms effective in the exchange of the chains between the micelles: chain insertion/expulsion and micellar merger/splitting. Their relative contributions are determined by the system variables: concentration, interaction parameter, and insoluble block size. In the relaxation of the chain exchange, the values of the eigenfrequencies revealed that the higher frequency modes of the relaxation come

from the chain insertion/expulsion mechanism. The micellar merger/splitting type of transitions led to the lower frequency eigenmodes of the relaxation. The latter type of transitions become more important at higher concentrations and less important (relative to the exchange via free chains) at higher interaction energies. Of course, the overall dynamics becomes slower as the energy of interaction of the insoluble block with the surroundings increases.

**Acknowledgment.** This research was supported by the National Science Foundation, Grants DMR 9220369 and INT 9312285.

### References and Notes

- (1) Procházka, K.; Bednář, B.; Mukhtar, E.; Svoboda, P.; Trěná, J.; Almgren, M. *J. Phys. Chem.* **1991**, *95*, 4563.
- (2) Wang, Y.; Balaji, R.; Quirk, R. P.; Mattice, W. L. *Polym. Bull.* **1992**, *28*, 333.
- (3) Wang, Y.; Kausch, C. M.; Chun, M.; Quirk, R. P.; Mattice, W. L. *Macromolecules* **1995**, *28*, 904.
- (4) Tian, M.; Qin, A.; Ramireddy, C.; Webber, S. E.; Munk, P.; Tuzar, Z.; Procházka, K. *Langmuir* **1993**, *9*, 1741.
- (5) Halperin, A.; Alexander, S. *Macromolecules* **1989**, *22*, 2403.
- (6) Aniansson, E. A. G.; Wall, S. N. *J. Chem. Phys.* **1974**, *78*, 1024.
- (7) Bednář, B.; Edwards, K.; Almgren, M.; Tormod, S.; Tuzar, Z. *Macromol. Chem., Rapid Commun.* **1988**, *9*, 785.
- (8) Wang, Y.; Mattice, W. L.; Napper, D. H. *Langmuir* **1993**, *9*, 66.
- (9) Haliloğlu, T.; Mattice, W. L. *Chem. Eng. Sci.* **1994**, *49*, 2851.
- (10) Haliloğlu, T.; Mattice, W. L. *Comput. Polym. Sci.* **1995**, *5*, 65.
- (11) Bahar, I.; Erman, B. *Macromolecules* **1987**, *20*, 1368.
- (12) Bahar, I.; Erman, B.; Monnerie, L. *Adv. Polym. Sci.* **1994**, *116*, 145.
- (13) Verdier, P. H.; Stockmayer, W. H. *J. Chem. Phys.* **1962**, *36*, 227.
- (14) Metropolis, N.; Rosenbluth, A. W.; Rosenbluth, M. N.; Teller, A. H. *J. Chem. Phys.* **1953**, *21*, 1087.
- (15) Haliloğlu, T.; Mattice, W. L. In *Solvent and Self-Assembly of Polymers*; Webber, S. E., Ed.; Kluwer: Dordrecht, in press.
- (16) Halperin, A.; Tirrell, M.; Lodge, T. P. *Adv. Polym. Sci.* **1992**, *100*, 31.

MA951301+